

# Spatiotemporal Evolution and Characteristics of Colluvial Landslide Deposits in Chutou Valley Based on Vegetation Analysis after Earthquake

Xiao Li

School of Construction Engineering, Jilin University, Changchun 130021, Jilin, China

**Abstract:** *The normalized vegetation index (NDVI) is a kind of index that characterizes vegetation development in a region. The level of NDVI can accurately reflect the development and distribution of vegetation, so it has a good and accurate indicator function in the study of vegetation. The research area of this paper is located in the mountainous area of southwest China with dense vegetation. Strong earthquake induced a large number of coseismic landslides, which not only caused serious damage to the vegetation in the region, but also caused secondary disasters such as debris flow as loose material sources. Therefore, this paper uses NDVI index to distinguish the significant differences between vegetation and deposit bodies, and obtains the evolution trend of vegetation in the study area since the Wenchuan earthquake in 2008. The evolution trend of vegetation is analyzed and compared with the results of optical remote sensing interpretation, and finally obtains the evolution law and characteristics of slide deposit bodies. Based on the above research results, NDVI is introduced into the evolution analysis of geological hazards, which provides scientific support for the analysis of debris flow source evolution by NDVI trend.*

**Keywords:** Remote sensing interpretation, NDVI, Debris flow, Landslide deposit body, Evolutionary analysis.

## 1. Introduction

Earthquake is an important inducement of landslide, especially in the strong earthquake, there will be a large number of coseismic landslide, which will seriously destroy vegetation and form a large number of landslide deposits. In the Wenchuan earthquake, it is estimated that about 40,000 to 50,000 deposits have been formed in the epicenter area [1]. Due to its unstable characteristics of loose accumulation, landslide deposits provide source conditions for post-earthquake secondary disasters such as post-earthquake landslide and debris flow, and have a great impact on post-disaster management and reconstruction.

The evolution of landslide deposits and secondary disasters is usually affected by a variety of factors, among which the coverage of vegetation and the recovery rate after damage are related to the occurrence density and quantity of geological disasters. Landslide will destroy vegetation, while debris flow will delay the recovery rate of vegetation, and loose landslide deposits will gradually decrease with the reinforcement of vegetation roots during recovery. Thus, the frequency of secondary disasters will be reduced [2][3]. Therefore, the long-term evolution trend of vegetation coverage can directly reflect the long-term evolution law of landslide deposits.

The normalized vegetation index (NDVI) is usually used as a representative index of the growth state of plants or vegetation coverage [4], so NDVI is more sensitive to the growth changes of vegetation in the study area [5]. It is difficult for vegetation to recover in a long period of time after being damaged, and the recovery rate does not change linearly with time, but dynamically changes according to the specific situation every year [6]. With the subsequent recovery of vegetation and the evolution of landslide deposits, NDVI will also have relative changes. By obtaining the time series NDVI from the earthquake to the present, the evolution law of the landslide deposit body can be obtained from the change law of NDVI.

Domestic and foreign scholars have used various methods to analyze the trend by using the time series NDVI data over the years. Jian et al. obtained the dynamic evolution trend of vegetation in the Qinghai-Tibet Plateau during 1982-2003 by using the single linear regression analysis [7]. Although linear regression analysis is simple and intuitive, and suitable for long-term evolution analysis, it ignores the complexity of vegetation evolution. Therefore, Xie et al. considered the comprehensive relationship between temperature, atmospheric precipitation and vegetation in analyzing the vegetation evolution trend of the Loess Plateau and adopted nonlinear regression analysis, and concluded that the vegetation evolution trend was different in different climate zones [8]. Although nonlinear regression analysis can more accurately reflect the evolution trend of vegetation in complex environments, it has high requirements on data and sample quality.

In addition, multi-spectral remote sensing image data can also be used for time series analysis. Liu et al conducted improved Mann-Kendall trend analysis (MMK) using AVHRR data set from 1982 to 2010, obtained the vegetation evolution trend of Weihe River basin in typical semi-arid and sub-humid climate zones, and analyzed the driving factors of the evolution [9]. Time series analysis can consider the vegetation evolution law of time and season factors, but the integrity and consistency of the data will affect the accuracy of the analysis results. When Militino analyzed the vegetation evolution in Spain from 1981 to 2015, he monitored the abrupt points of vegetation evolution and obtained four types of regional evolution trends with different NDVI values [10]. Although the monitoring of mutation points can clearly identify the driving factors of vegetation change, the selection of mutation points is relatively subjective and not sensitive enough to the slowly evolving vegetation. Therefore, Zhao et al proposed a Bayesian estimation model (BEAST) to extract the dynamics of multi-scale nonlinear ecosystem. Through the combination of multiple models, It can be used to detect robust change

points and conduct nonlinear trend analysis, so as to explore the dynamic evolution trend and driving factors of vegetation by combining multiple factors with time series data [11].

Based on remote sensing data from 2007 to 2023, visual interpretation and extraction of normalized vegetation index (NDVI) were carried out to analyze the change characteristics of vegetation coverage and landslide deposits in the area 15 years after the earthquake, and the long-term evolution law of landslide deposits in the area was obtained. The landslide activity in Chutougou was close to the pre-earthquake level. However, a large number of landslide deposits in the gully still have the possibility of inducing debris flow again.

## 2. Overview of the Research Area

### 2.1 Geographical Location

The research area is mainly located in the territory of Miansi town, Wenchuan County. The main traffic routes around Miansi town include Duwen Expressway and G213 National Highway, which start from Chengdu and extend to the surrounding areas through Wenchuan County. They are the most important traffic routes in Aba Prefecture. It is located in the southwest direction of Wenchuan County, about 18km away from Wenchuan County and 32km away from Yingxiu Town, the epicenter of Wenchuan earthquake (Figure 1).

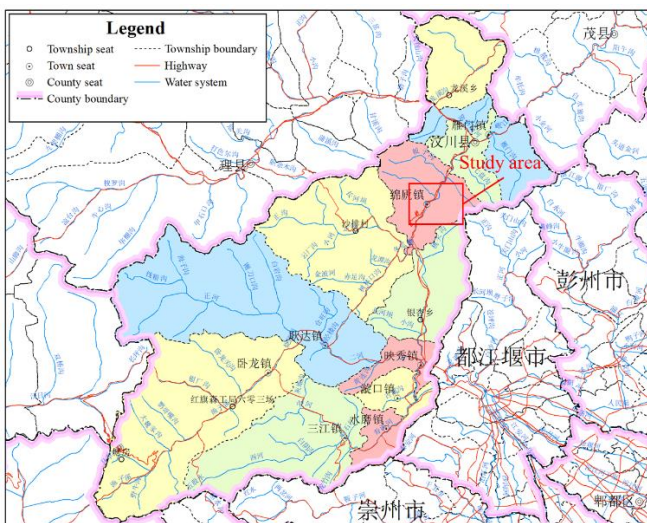


Figure 1: Geographical location map of the research area

### 2.2 Topography and Landform

The overall topography of the basin in the study area is high in the south and low in the north, which is a hilly landform with serious erosion. There is a large elevation difference in the basin. The lowest point is at the junction between Chutou Gully mouth and Minjiang River, with a height difference of 2,952m from the top to the bottom of the gully. The study area is the largest debris flow gully in the basin, with an area of 21.7km<sup>2</sup> and the main gully length of 8.9km. Due to the large elevation difference, the rock slope and rock wall in the area are steep, and the loose deposits at the top of the slope are easy to flow to the bottom of the ditch and converge, providing the source conditions for debris flow.

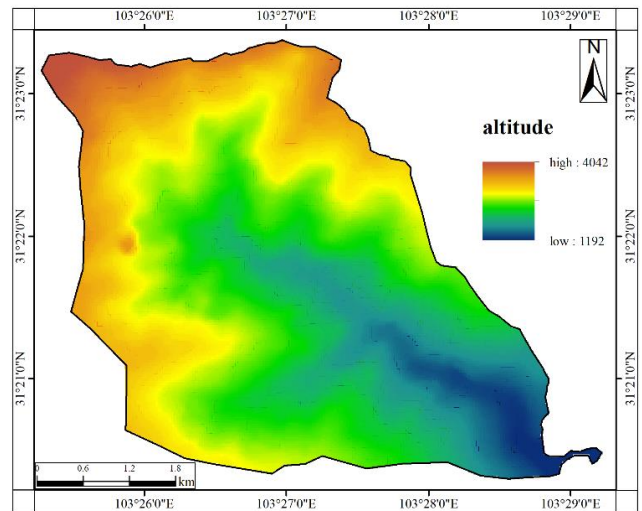


Figure 2: Elevation distribution map of the research area

### 2.3 Geological Structure and Stratigraphic Lithology

The research area is located in Jiudingshan Cathaysian tectonic belt, in which the main fault structures include Maowen fault belt and Jiudingshan fault belt. The Maowen fault zone is a northeast-striking large compressive fault. The fault strikes northeast-30°~45°, the total is about 40°, the dip is 300°~330°, the dip Angle is 45°~80°, and the length is 156km. Jiudingshan fault zone is the largest branch fault of Maowen fault, and it is a compression-torsion inclined thrust fault. The strike is 40°~50° to the northeast, the fault is 56km long, the dip is 305°~315°, the fault line bends and extends, the dip Angle is 10°~74°, and the fault plane occurrence becomes steeper.

The strata in the study area are mainly acidic magmatite ( $\gamma$ ), diorite ( $\delta_2$ ), Proterozoic Huanghuangshui Group ( $P_{thn}$ ), Silurian Maoxian Group ( $S_{mx}$ ), and plagiogranite ( $\gamma_{02}^{(4)}$ ) of the 4th Jinning Age.

### 2.4 Meteorological and Hydrological Conditions

According to the observation of Weizhou meteorological station in 23 years, the average annual precipitation is 526.3mm. The rainfall in this area varies greatly from year to year, and the annual distribution is not uniform. Concentrated rainfall usually occurs from May to August, which provides sufficient water conditions for the occurrence of debris flow. At the same time, the time curve of disaster development in the region is basically consistent with the distribution of precipitation.

Minjiang River is the main river in the region. It originates from the southern foot of Minshan Mountain, passes through Songpan and Maoxian County, flows into Wenchuan from the northeast of the county, and runs through the eastern part of Wenchuan. The flow length of Minjiang River is 88 km with a basin area of 1,428.476 km<sup>2</sup>. The valley is deep, the current is swift, and the average gradient of the river bed is 8‰. The annual average discharge ranges from 168 to 268 m<sup>3</sup>/s. The groundwater is mainly composed of pore water of quaternary loose accumulation layer and bedrock fracture water, but no karst water is found. The main recharge way is atmospheric precipitation and surface water.

### 3. Data Sources

Select 2m high-resolution optical images of Google Earth platform from 2007 to 2023. Aiming at the extraction of NDVI data set, this paper uses the remote sensing images of Landsat series satellites for time series analysis. In the past 50 years of earth observation, Landsat series satellites have provided a large number of long-term continuous complete remote sensing data for research. In this study, 30m precision

multi-spectral remote sensing data of Landsat-7 and Landsat-8 satellites were selected from the Earthdata platform of NASA for analysis. At the same time, the study area often has cloud cover in summer (from June to September) and snow cover in winter and spring (from November to March), so the Landsat series of multi-spectral remote sensing images with cloud cover less than 10% in summer and autumn were selected.

**Table 1:** Selected remote sensing images

Remote sensing image date	20070419	20080523	20090814	20100427	20110719	20131207	20140601	20150212
Select satellite	Landsat-7ETM+					Landsat-8OLI		
Remote sensing image date	20160318	20170406	20180409	20190311	20200414	20210604	20220420	20230415
Select satellite	Landsat-8OLI							
Remote sensing image date	2007	2008	2011	2014	2015	2018	2019	2021
Select satellite	Google Earth high-resolution Remote sensing imagery (level 16)							

### 4. Data Processing

#### 4.1 Optical Remote Sensing Interpretation

Google Earth high-resolution remote sensing images were used to visually interpret the slide deposits in the study area. A large number of geological disasters such as landslide accompanied by strong earthquakes often cause great damage to vegetation. Therefore, landslide deposits can be distinguished according to the difference in tone, texture and surface markers of remote sensing images. Landslide deposits usually have a distinct boundary with vegetation, which is yellowish to grayish white, and are loosely deposited initially. Over time, they may be covered by vegetation or slide down the slope to the bottom of the ditch. High-resolution optical image interpretation can be completed according to the characteristics.

Considering the remote location and early research period of the study area, slow data update, complex terrain, frequent cloud cover in summer and other limitations of data sources, the interpretation information of each phase was compared with that of the previous phase for superposition analysis, so as to obtain the changes in the quantity and area distribution of each phase of remote sensing image compared with that of the previous phase. At the same time, the distribution density of the landslide deposit body was analyzed and calculated, and the evolution trend of the landslide deposit body after the earthquake was obtained from three aspects: distribution density, distribution quantity and distribution area.

#### 4.2 Analysis of Vegetation Coverage

Landslide will cause serious damage to vegetation and form a large number of loose landslide deposits. These loose deposits will not only destroy buried vegetation formations, but also become new debris flow sources and form new debris flow in the intensive rainfall season in the study area. Therefore, the recovery of vegetation will also directly affect the attenuation of landslide deposits and debris flow sources. The red band and near infrared band of Landsat data were used to calculate NDVI in the study area, and then the vegetation coverage (FVC) was calculated, and the vegetation recovery situation in the study area was studied through the changes of FVC over

the years. ENVI 5.3 was used to extract NDVI from remote sensing images in Landsat time series data to further obtain the vegetation coverage in the study area. The basic formula is as follows:

$$NDVI = \frac{NIR-RED}{NIR+RED} \quad (1)$$

$$FVC = \frac{NDVI-NDVI_{soil}}{NDVI_{veg}+NDVI_{soil}} \quad (2)$$

Normalized vegetation index NDVI can be extracted according to band calculation. For the treated NDVI values in the study area, the empirical value confidence interval is selected, and the NDVI value with a confidence interval of 95% is regarded as the vegetation index  $NDVI_{veg}$  with complete vegetation coverage, and the NDVI value with a confidence interval of 5% is regarded as the vegetation index  $NDVI_{soil}$  with complete bare land. At the same time, considering that the NDVI value of the bare soil end element is -0.1-0.2, and the NDVI value of the pure vegetation end element is above 0.8, the selection of the pure bare soil value entirely based on the confidence interval may produce a lower pure vegetation value, resulting in inaccurate [12] results. Therefore, after obtaining the  $NDVI_{veg}$  and  $NDVI_{soil}$  values over the years in combination with the seasons of the study area, the vegetation coverage of the study area can be calculated by using the bands.

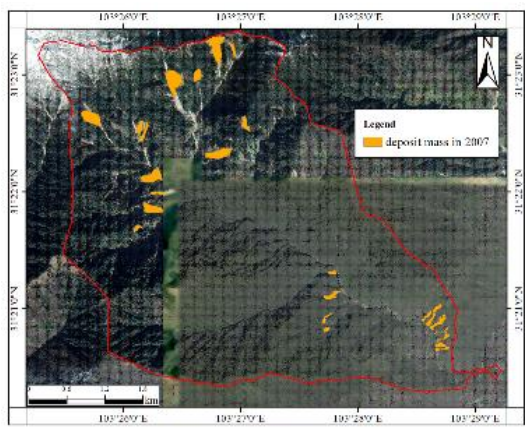
The distribution of vegetation coverage calculated by remote sensing images in each phase was compared. By comparing the changes of vegetation coverage over the years, the vegetation recovery over the years could be intuitively seen, and then the evolution of landslide deposits could be known.

#### 4.3 Analysis of Topographic Factors

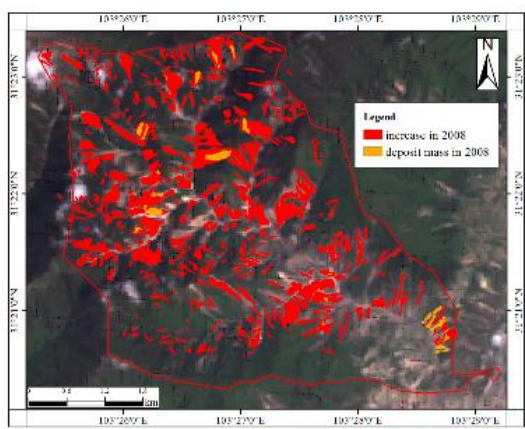
Due to the overall inclination of the basin with a large elevation difference, the elevation in the basin can be used as the main influencing factor for the formation and migration of landslide deposits, and the slope and slope are the influencing factors for the growth and development of vegetation [13]. Therefore, the height, slope and slope distribution of the hoe ditch are calculated using the STRM 30m precision elevation data obtained from the USGS. The optical interpretation results were manually classified to obtain the evolution of slide deposits in different regions.

## 5. Results and Discussion

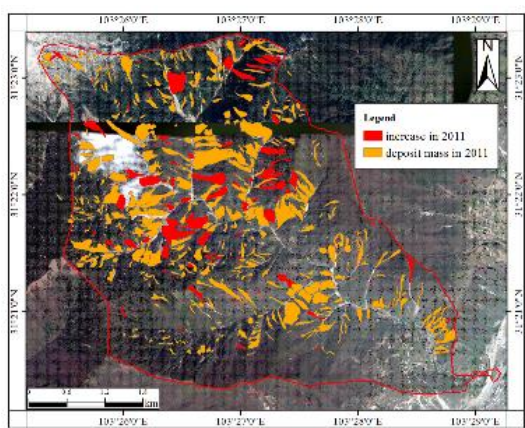
### 5.1 Evolution of Collapsible Deposits



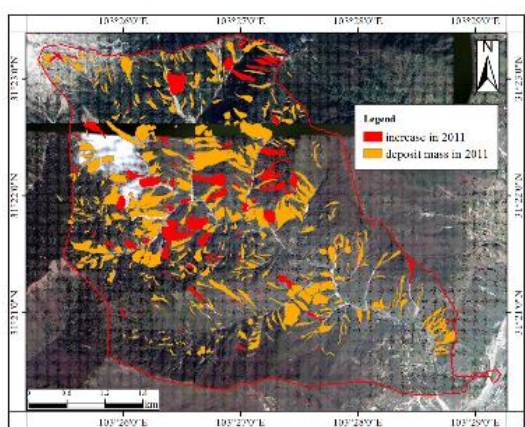
2007



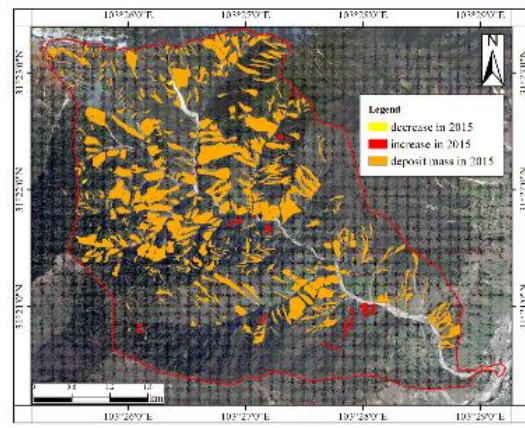
2008



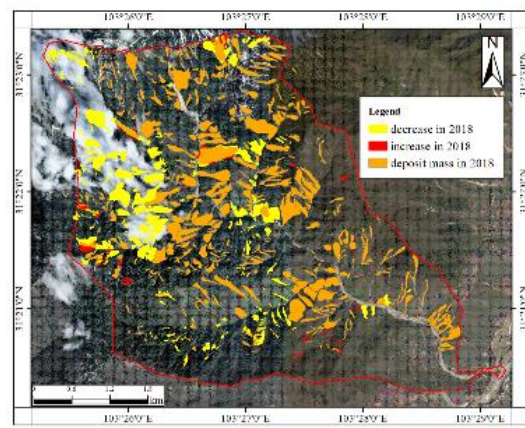
2011



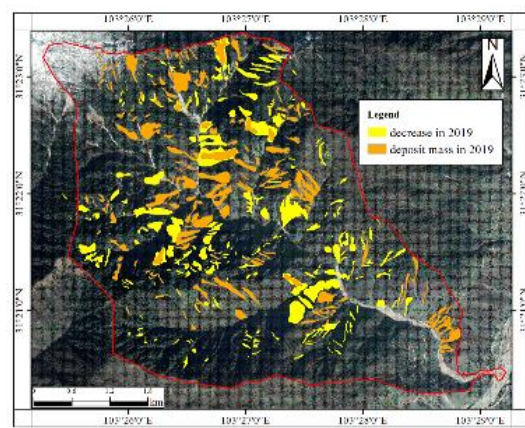
2014



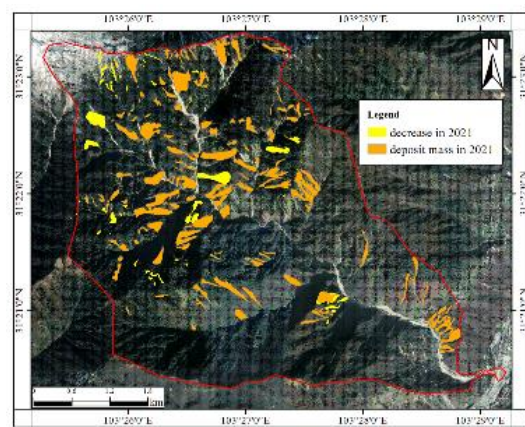
2015



2018



2019



2021

Figure 3: Result of interpretation of slide deposits over the years

In the visual interpretation analysis based on high-resolution optical remote sensing images of Google Earth, there were only about 20 landslide deposits in Chutou Ditch before the earthquake, and the distribution was relatively scattered, but the vegetation in the ditch was dense and the overall state was stable. After the 2008 earthquake, there were 394 landslide deposits distributed in the whole ditch. It is speculated that the strong vibration made the whole ditch in an unstable state, which was proved by the large increase in the number of landslide deposits in 2011. Under the influence of strong shaking, steep terrain in the gully and the concentrated precipitation in Wenchuan in summer, new secondary geological disasters continued to occur, which made the number of landslide deposits rise to about 479 in the years after the earthquake, with an increase rate of 20%.

According to the visual interpretation results in 2014 and 2015, the number of landslide deposits began to decrease. Due to the continuous accumulation of a large number of loose material sources in the ditch, large-scale debris flow disasters were finally induced in 2013 and 2014, and about  $70 \times 10^4 \text{m}^3$  solid materials were washed out in the two debris flows [14], causing serious damage. A large amount of alluvial accumulated from the flow area to the vicinity of the gully. The debris flow carried away a large number of loose landslide deposits and seriously damaged the development of vegetation, so the number of interpretive materials remained basically unchanged in 2014 and 2015. In 2018, it can be seen that the number of landslide deposits dropped to about 380, which is close to the number after the earthquake in 2008, but it dropped to about 308 after another very large scale debris flow occurred in 2019. About  $75 \times 10^4 \text{m}^3$  solid material was expelled from this debris flow [14], which is greater than the sum of the mass of debris expelled from the previous two debris flows. Therefore, the number of landslide accumulation bodies has a rapid decline trend. Due to the large-scale debris flow disaster in Chutou again in 2020, the number of landslide deposits dropped rapidly again to about 166 after 2021.

Due to the remote location of Chutou Ditch and slow image updating, it is necessary to combine relatively continuous NDVI data to obtain the annual temporal evolution of vegetation. However, through the corresponding analysis between the optical image interpretation results and the eruption time nodes of several debris flows in Chutou Ditch, it is found that with the outbreak of four debris flows, the amount of loose material sources in the ditch decreases, and the number of slide deposits also decreases. After the occurrence of debris flow in 2013 and 2014, the number of landslide deposits began to decline continuously, and accelerated to decline after the outbreak of extremely large debris flow in 2019 and large debris flow in 2020, indicating that landslide deposits are the main source of debris flow in Chutou Ditch, and it can be concluded that the reduction of the number of landslide deposits is directly related to the reduction of provenance quantity. Therefore, about 166 landslide deposits interpreted in 2021 can indicate that there is still a considerable amount of loose material sources in Chutou Ditch, so large-scale debris flow disasters may occur again under strong precipitation conditions.

### 5.2 Sliding Deposits and Topographic Factors

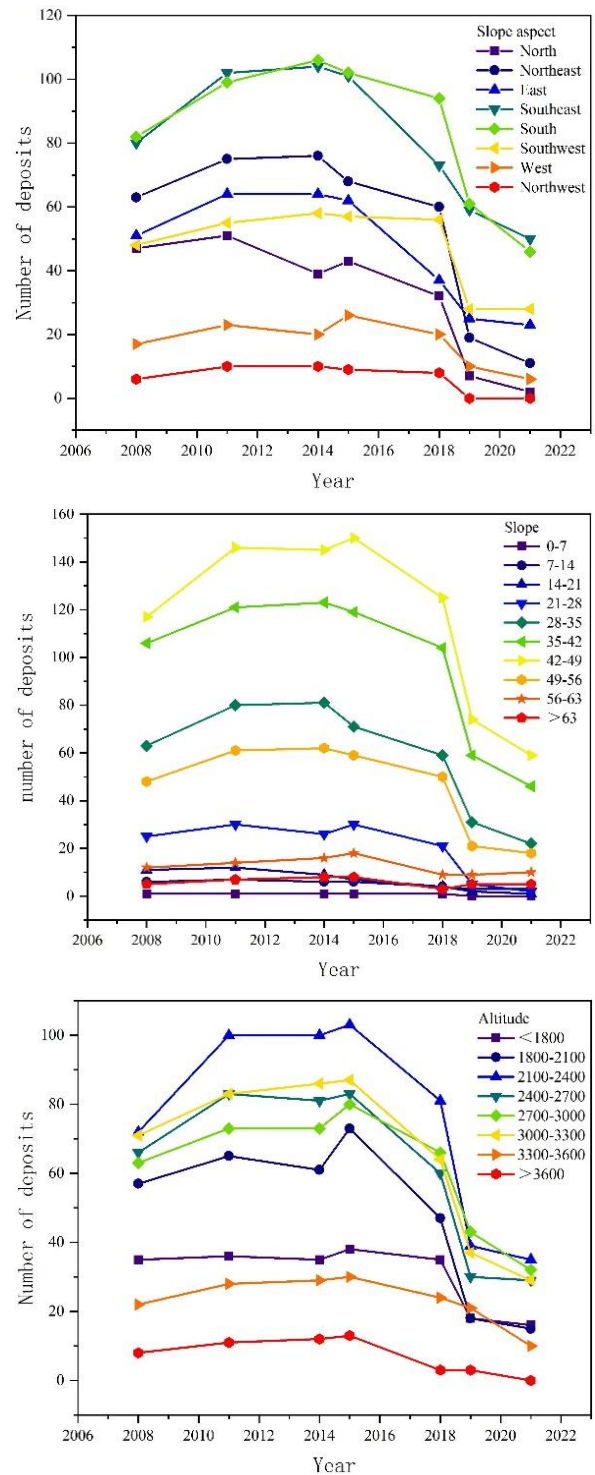


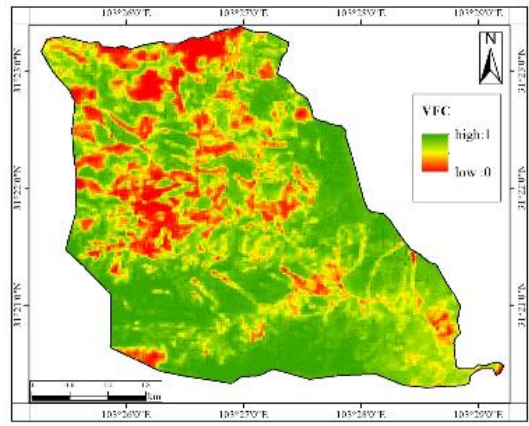
Figure 4: Statistical distribution map of deposits under different topographic factors

### 5.3 Vegetation Coverage

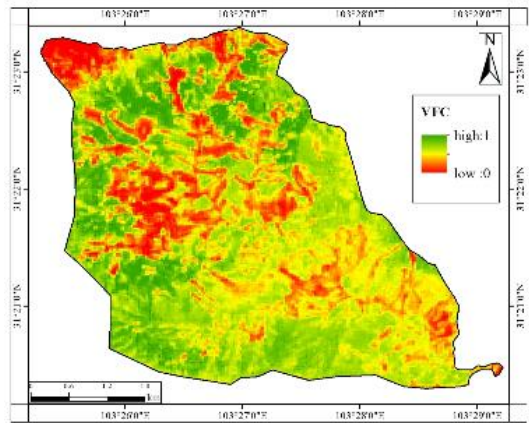
Through Landsat data with a precision of 30m, although NDVI with no or few clouds can be obtained in the past years since 2007, the study area is remote and the climate is cloudy all the year round, so only NDVI and vegetation coverage evolution with year as the minimum time scale can be obtained.

Topographic factors are related to the distribution and quantity of accumulations. According to the classification of landslide deposits according to slope, slope direction and elevation, the time evolution trend chart is generated. It can be

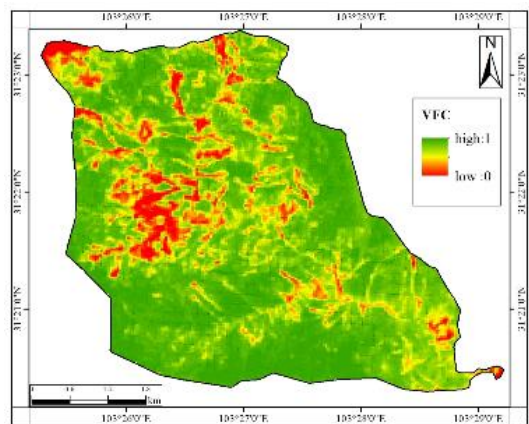
seen that the general trend is gradually increasing before 2014 and rapidly decreasing after 2014. According to the quantity distribution of landslide deposits, landslide deposits are mainly distributed in the N-NE slope direction and the slope range of  $35^{\circ}\sim 49^{\circ}$ . Within the elevation range of 1800m~3300m. Because the hoe ditch is high in the north and low in the south as a whole, the landslide is more likely to occur in the south, and the accumulation body is formed, and the hoe ditch branch is located at the foot of the south slope. According to the chart, the accumulations in all areas showed a rapid decline after 2018, and tended to be stable after 2019, indicating that the huge debris flow in 2019 carried away a large number of sliding accumulations, resulting in a steep decline in the number of accumulations. At the same time, there are still some terrain with small changes in the number of landslide deposits. For example, in areas with flat slope ( $< 14^{\circ}$ ) and steep slope ( $> 56^{\circ}$ ), the number of landslide deposits has remained basically unchanged since the earthquake. The main reason is that areas with steep slope are usually located at the top of steep slope or at high altitude, so the recovery is slow. The flat slope area is usually located near the bottom of the ditch in the area susceptible to landslide and debris flow, which is easy to induce the formation of new accumulation bodies again. The area with higher elevation ( $> 3000\text{m}$ ) is mainly located at the rear of the steep slope at the top of Chutou gully, so the recovery is slow. At the same time, the landslide deposits in this area are not easy to be scour by debris flow and become the source, so the number is not affected by the evolution of large-scale debris flow.



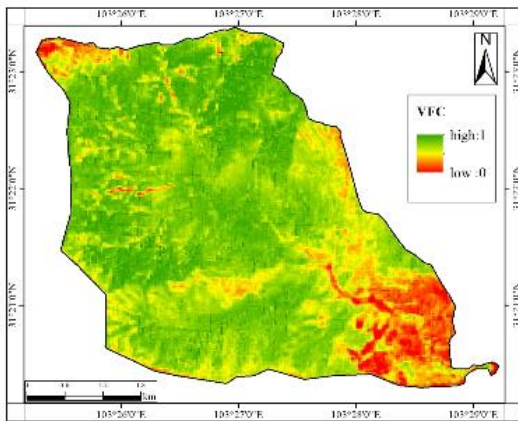
2009(Summer)



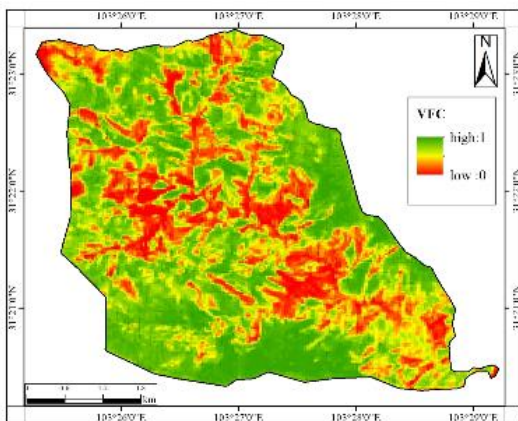
2010



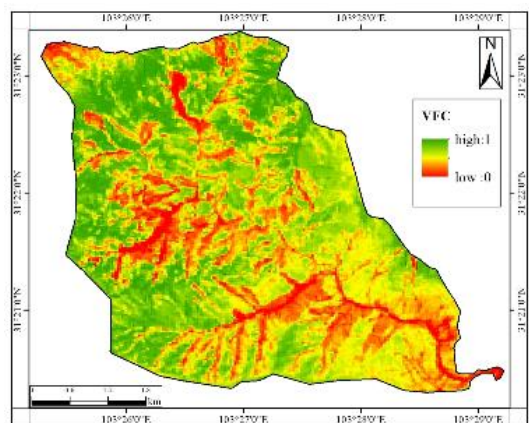
2011(Summer)



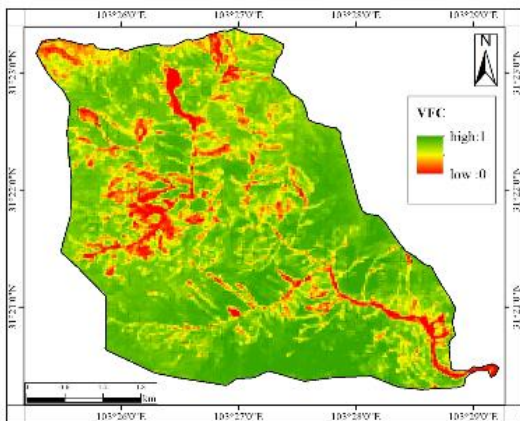
2007



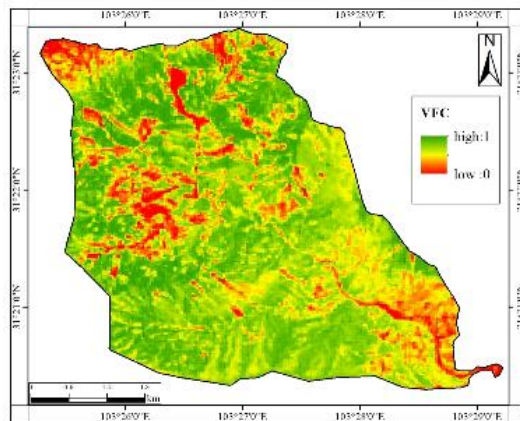
2008



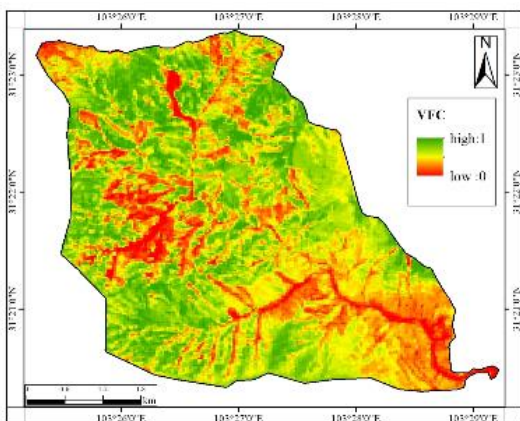
2013



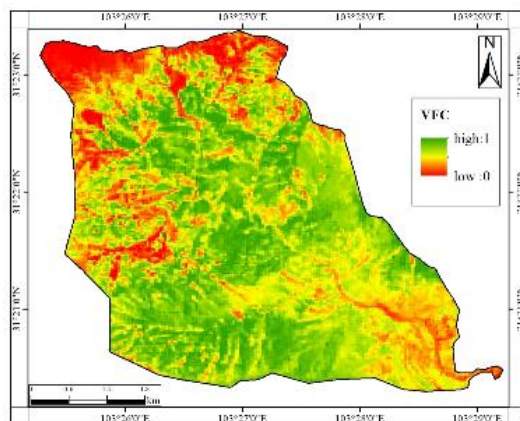
2014(Summer)



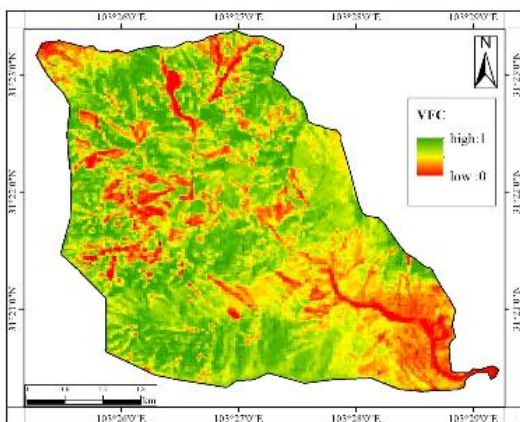
2018



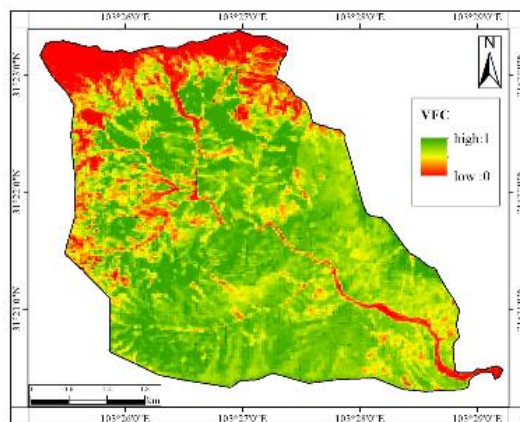
2015



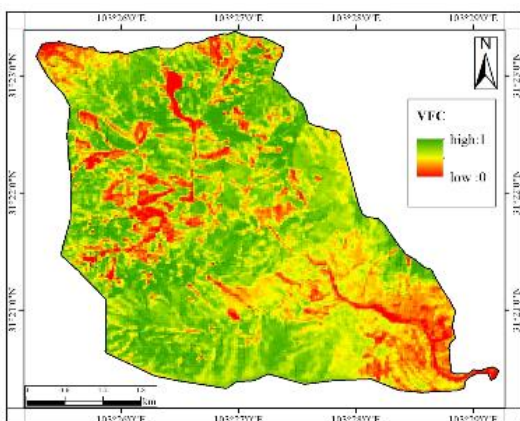
2019



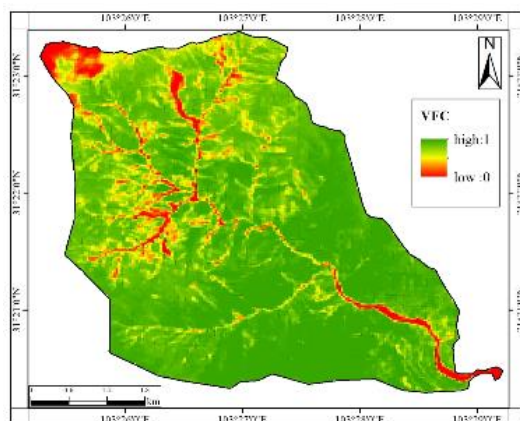
2016



2020



2017



2021(Summer)

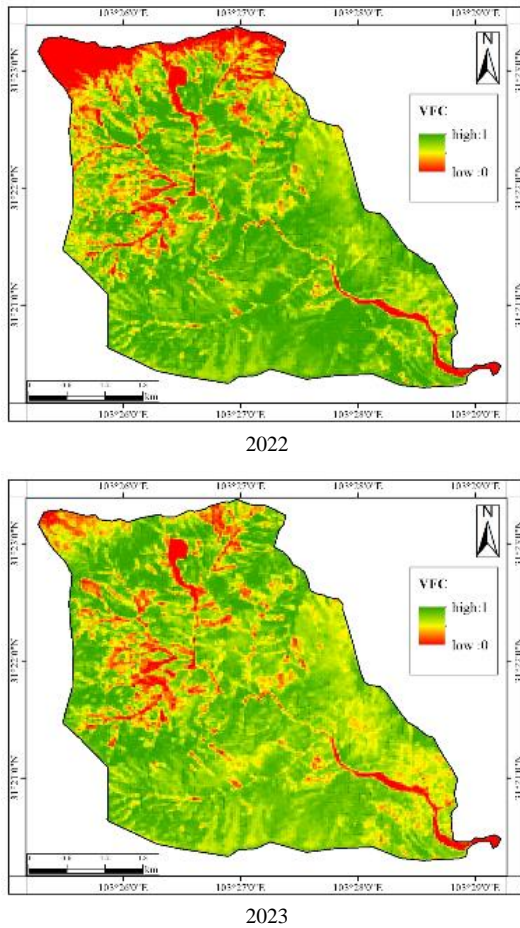


**Figure 5:** Vegetation cover evolution over the past years

According to the analysis of the obtained vegetation coverage, the overall vegetation coverage in the Chutou Ditch area was good in 2007. Compared with the south slope, the vegetation coverage in the north slope was relatively sparse, and the area at the mouth of the ditch and the bottom of the main ditch were basically bare land. The remote sensing images selected in 2008 were taken shortly after the earthquake. It can be seen that the vegetation in the gully was seriously damaged, the overall vegetation coverage in the gully decreased significantly, and the area with near zero coverage could be seen as the area where the landslide accumulative body developed. 2009, 2011 and 2014 were the summer vegetation coverage. Through the comparison of the distribution of vegetation coverage from 2009 to 2011, it can be seen that although some vegetation covered the accumulative body area in summer, the area of sliding accumulative body continued to increase, that is, the region was in an unstable state. From 2013 to 2014, the coverage at the mouth of the gutou ditch decreased significantly compared with that before. Some loose deposits accumulated in the gully due to the influence of rainfall and slope, and the deposit area at the top of the slope decreased, indicating that a large number of sliding deposits accumulated at the mouth of the gutou ditch along with two large debris flows in 2013 and 2014. After 2015, it can be seen that the area with low vegetation coverage began to gradually decrease, the area with vegetation coverage close to the bare land also decreased from 2015, and the overall vegetation coverage in the region gradually increased. In summary, the overall stability of the study area has been stabilized since 2015, and the landslide deposits in the ditch have gradually decreased over time. Compared with the vegetation coverage

in 2019 and 2020, the overall vegetation coverage was significantly increased, but the vegetation coverage from the bottom of the channel to the mouth of the channel in the circulation area decreased to close to zero, indicating that a large number of deposits were washed here after 2019, and the vegetation further recovered. The change of FVC in 2020 tends to be stable again, which is the same as the result of visual remote sensing interpretation.

Based on the FVC extracted from the above calculation, the change trend of FVC in the study area from 2008 to 2023 can be calculated by referring to the one-element linear regression analysis equation of previous studies [15].

$$S_{\text{slope}} = \frac{\left[ n \times \left( \sum_{k=1}^n k \right) \times x_k \right] - \left( \sum_{k=1}^n k \right) \times \left( \sum_{k=1}^n x_k \right)}{\left( n \times \sum_{k=1}^n k^2 \right) - \left( \sum_{k=1}^n k \right)^2} \quad (3)$$

In this paper, unitary linear regression analysis is adopted to conduct Slope trend analysis and significance test on the time series data, and the slope slope slope and significance coefficient p of the calculated FVC over the past years are divided. Six grades were divided according to slope > 0 as increase, slope < 0 as decrease, p < 0.01 as extremely significant, 0.01 < p < 0.05 as more significant, and p > 0.05 as non-significant.

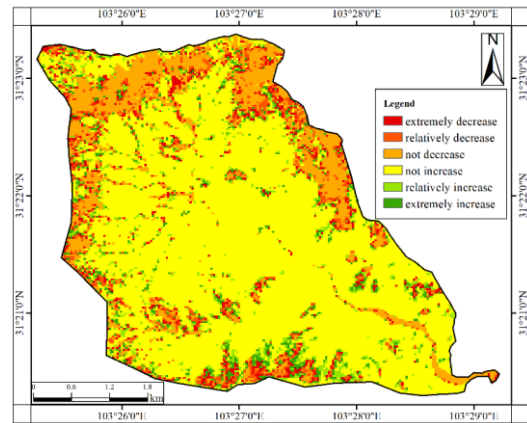


**Figure 5:** Trend chart of vegetation coverage change from 2008 to 2023

According to the change trend in Fig. 5, it can be seen that for the areas with extremely increase to relatively increase, vegetation is in the stage of rapid development, and the area of accumulations gradually decreases, and the area with extremely increase is the area of the collapse accumulations. Therefore, it can be seen that vegetation is recovering in the above areas. For the areas without significant change, the vegetation coverage has been relatively stable; for the areas without significant increase, the vegetation coverage has been restored to close to the pre-earthquake coverage after the damage, and the vegetation change in these areas is no longer significant. For the areas without significant reduction in the trench, the vegetation has not recovered in these areas, but the sliding accumulative body has tended to be stable, and the area increase will not be further caused by secondary disasters. The area with no significant increase or decrease basically covers the whole study area, indicating that the whole area is basically stable at present, and only a few areas with significant decrease to significant decrease remain, which are the areas with the increase of the area of slide deposits. The area with an increase is mainly located in the southern part of



the study area and belongs to the position near the river. Considering its influence, slide deposits are more prone to slide than other areas. The remaining areas are scattered and scattered, and the significantly reduced areas are the noise caused by cloud interference.

According to the above analysis of the evolution trend of vegetation coverage, it can be seen that vegetation has basically recovered in Chutougou area, the whole study area has remained stable, and no new sliding deposits are produced. Based on the distribution of vegetation cover change trend and the distribution of slide deposits interpreted by optical remote sensing, the evolution of slide deposits in Chutougou Basin can be analyzed. At present, most of the slide deposits are distributed in the gully mouth and the bottom of the main gully, and the deposits in the upstream branch gully are gradually reduced and covered by vegetation, so the vegetation coverage in the gully formed area remains stable. Compared with the flow area, the formation area is located in a higher terrain, and the climatic conditions of the Chutou Valley will make the precipitation concentrate in a few months, thus satisfying the provenance, water source and topographic conditions required for the occurrence of debris flow at the same time. Therefore, the Chutou Valley evolved into a debris flow valley after the earthquake. According to the investigation of the history of debris flow in Chutou area, it can be seen that four large-scale debris flow occurred in Chutou since the earthquake, which occurred in 2013, 2014, 2019 and 2020 respectively. Repeated debris flows left a large amount of deposits from the flow area to the mouth of the gully, and the occurrence of debris flows also induced the recurrence of landslides near the gully, forming new landslide deposits and destroying vegetation, so the vegetation coverage from the flow area to the mouth of the gully was always low.

## 6. Conclusion

The general evolution trend of landslide deposits in Chutougou area is that they were in a stable state before the 2007 earthquake. Before the earthquake, the vegetation was abundant and the rock mass structure was stable, and geological disasters such as landslide and landslide rarely occurred in Chutougou area. After the 2008 earthquake, the landslide deposits became the main source of the re-start of debris flow in Chutougou area, and the decay rate of landslide in Chutougou area was slow. Before 2013, the sliding accumulation body was in a gradually increasing state, which induced two debris flow disasters in 2013 and 2014. After that, the area gradually became stable and vegetation began to recover at an accelerated pace, but there were still a large number of landslide deposits, which induced two debris flow disasters in 2019 and 2020. According to the recovery trend of vegetation coverage and visual interpretation analysis, the landslide activity in Chutou was close to the pre-earthquake level. However, a large number of landslide deposits in the ditch still have the possibility of inducing debris flow again.

## References

[1] Cui P, Lin Y M, Chen C. Destruction of vegetation due to geo-hazards and its environmental impacts in the

- Wenchuan earthquake areas. [J]. *Ecological Engineering*, 2012,44 (7): 61-69
- [2] Guo Changbao, Du Yuben, Zhang Yongshuang, Zhang Guangze, Yao Xin, WANG Ke, Liu Jian. Development characteristics of geological hazards and formation mechanism of typical landslides in Xianshuihe fault zone, western Sichuan [J]. *Geological Bulletin of China*,2015,34(01):121-134.
- [3] Huang Runqiu, Fan Xuanmei. The landslide story [J]. *Nature Geoscience*,2013,6(5):325-326.
- [4] Shao Quanqin, Fan Jiangwen, Liu Jiyuan, et al. Assessment on the effects of the first-stage ecological conservation and resto. ration project in Saniiangyuan Region, *Acta Geographica Sinica*, 2016. 71(1): 3-34.1. DOI: 10.11821/dlxb201601001.
- [5] Huang XL, Zhang T B, YiG H, et al. Dynamic changes of NDVI in the growing season of the Tibetan Plateau during the past 17 years and its response to climate change [J]. *International Journal of Environmental Research and Public Health*, 2019, 16(18): 3452-3472.
- [6] WANG Feilong, Chen Ming, Wang Xiaodi, Ding Jun, Zhang Hao. Wenchuan earthquake epicenter areas collapse the vegetation recovery and long-term effects of the [J]. *Journal of soil and water conservation bulletin*, 2020,40(03):175-179.DOI:10.13961/j.cnki.stbctb.2020.03.025.
- [7] Jian Peng, Zhenhuan Liu, Yinghui Liu, Jiansheng Wu, Yinan Han, Trend analysis of vegetation dynamics in Qinghai-Tibet Plateau using Hurst Exponent, *Ecological Indicators*, Volume 14, Issue 1, 2012, 28 Pages - 39, ISSN 1470-160 - x, <https://doi.org/10.1016/j.ecolind.2011.08.011>.
- [8] Xie, B., Jia, X., Qin, Z. et al. Vegetation dynamics and climate change on the Loess Plateau, China: 1982-2011. *Reg Environ Change* 16, 1583-1594 (2016). <https://doi.org/10.1007/s10113-015-0881-3>.
- [9] Saiyan Liu, Shengzhi Huang, Yangyang Xie, Hao Wang, Qiang Huang, Guoyong Leng, Pei Li, Lu Wang, Spatial-temporal changes in vegetation cover in a typical semi-humid and semi-arid region in China: Changing patterns, causes and implications, *Ecological Indicators*, Volume 98, 2019, Pages 462-475, ISSN 1470-160 - x, <https://doi.org/10.1016/j.ecolind.2018.11.037>.
- [10] Militino, A.F., Ugarte, M.D., Perez-Goya, U. (2018). Detecting Change-Points in the Time Series of Surfaces Occupied by Pre-defined NDVI Categories in Continental Spain from 1981 to 2015. In: Gil, E., Gil, E., Gil, J., Gil, M. (eds) *The Mathematics of the Uncertain. Studies in Systems, Decision and Control*, vol 142. Springer, Cham.
- [11] Kaiguang Zhao, Michael A. Wulder, Tongxi Hu, Ryan Bright, Qiusheng Wu, Haiming Qin, Yang Li, Elizabeth Toman, Bani Mallick, Xuesong Zhang, Molly Brown, Detecting change-point, trend, and seasonality in satellite time series data to track abrupt changes and nonlinear dynamics: A Bayesian ensemble algorithm, *Remote Sensing of Environment*, Volume 232, 2019, 111181, ISSN 0034-4257. <https://doi.org/10.1016/j.rse.2019.04.034>.
- [12] Montandon L M, Small E E. The impact of soil reflectance on the quantification of the green vegetation

- fraction from NDVI - ScienceDirect [J]. *Remote Sensing of Environment*, 2008, 112(4):1835-1845.
- [13] HU Shenjuan, HU Juanjuan, ZHENG Yeshe, et al. Inner Mongolia ecological barrier area vegetation change and precipitation, the influence of temperature on the [J]. *Journal of northeast forestry university*, 2023, 51(12): 44-50+80.DOI:10.13759/j.cnki.dlxb.2023.12.002.
- [14] Fan, X., Scaringi, G., Domenech, G., Yang, F., Guo, X., Dai, L., He, C., Xu, Q., and Huang, R.: Two multi-temporal datasets that track the enhanced landsliding after the 2008 Wenchuan earthquake, Earth price. *Sci. Data*, 11, 35-55, <https://doi.org/10.5194/essd-11-35-2019>, 2019.
- [15] Zhang Y Y, Zhong L, Fan X Y, et al. Minjiang river valley hoe ditch earthquake debris flow hazard -formative model [J]. *Journal of mountain*, 2021, 39(05): 756-766.DOI:10.16089/j.cnki.1008-2786.000636.